



A Geometrical Theory for Spiral Waves in Excitable Media

Author(s): James P. Keener

Source: *SIAM Journal on Applied Mathematics*, Vol. 46, No. 6 (Dec., 1986), pp. 1039-1056

Published by: Society for Industrial and Applied Mathematics

Stable URL: <http://www.jstor.org/stable/2101658>

Accessed: 07-06-2018 15:17 UTC

JSTOR is a not-for-profit service that helps scholars, researchers, and students discover, use, and build upon a wide range of content in a trusted digital archive. We use information technology and tools to increase productivity and facilitate new forms of scholarship. For more information about JSTOR, please contact support@jstor.org.

Your use of the JSTOR archive indicates your acceptance of the Terms & Conditions of Use, available at <http://about.jstor.org/terms>



Society for Industrial and Applied Mathematics is collaborating with JSTOR to digitize, preserve and extend access to *SIAM Journal on Applied Mathematics*

A GEOMETRICAL THEORY FOR SPIRAL WAVES IN EXCITABLE MEDIA*

JAMES P. KEENER†

Abstract. In this paper, we develop a geometrical theory for waves in excitable reacting media. Using singular perturbation arguments and dispersion of traveling plane wave trains, we derive an approximate theory of wave front propagation which has strong resemblance to the geometrical diffraction theory of high frequency waves in hyperbolic systems, governed by the eikonal equation. Using this theory, we study the effect of curvature on waves in excitable media, specifically, rotating spiral patterns in planar regions. From this theory we are able to determine the frequency and wavelength for spiral patterns in excitable, nonoscillatory media.

Key words. spirals, excitable media

AMS(MOS) subject classifications. 35K57, 92A09

1. Introduction. Geometric diffraction theory has been very successful in providing approximate (asymptotic) solutions for wave propagation problems in hyperbolic systems [8], [15], [16]. These techniques, also known as ray tracing, are currently used in a wide variety of applications in geophysics and electromagnetic theory.

The advantage of geometrical optics is that one can get direct approximate information about wave propagation in a variety of media in the asymptotic limit of high frequency waves from equations that are substantially easier to solve than the full system of equations. The loss, of course, is that as in any approximate theory, there are situations where the approximate solutions fail to produce accurate results.

In recent years, it has been shown that systems of nonlinear parabolic equations can have solitary waves and periodic wave trains. Typical examples describe propagation of electrical activity in neural tissue [6], [7], [12], [25], [33] and waves of chemical activity in the Belousov-Zhabotinskii reaction [32]. Equations modeling these phenomena are necessarily complicated. Exact analytical solutions are virtually impossible to find and numerical solutions of stiff equations in higher dimensional media are difficult and costly to obtain. The value of an approximate analytical theory is evident.

In this paper we develop a geometrical theory for waves in excitable media. The theory is asymptotic since it applies in the limit that the excitable dynamics evidence multiple time scales, and wave fronts occur as sharp transitions (boundary layers) between slowly varying regions. This is in direct analogy with the weak shock approximation of geometrical optics in hyperbolic problems.

In the next section we review singular perturbation theory and dispersion of waves in one spatial dimension. In § 3 we extend this theory to waves in two dimensions. Finally in § 4 we apply this theory to rotating patterns in two dimensions and show how wavelength and propagation speed are determined. Further use of this theory to other problems will appear in forthcoming papers.

* Received by the editors April 15, 1985, and in revised form January 21, 1986. Portions of this research were performed at the Centre for Mathematical Biology, Oxford University, supported by the Science and Engineering Research Council of Great Britain GR/C/63595, and at the Mathematics Research Branch of the National Institute of Arthritis, Diabetes and Digestive and Kidney Diseases, National Institutes of Health. Additionally, this work was partially supported by National Science Foundation grant MCS83-01881.

† Department of Mathematics, University of Utah, Salt Lake City, Utah 84112.

2. Wave propagation and dispersion. As a model problem, we consider the equations

$$(2.1) \quad \varepsilon \frac{\partial u}{\partial t} = \varepsilon^2 D \nabla^2 u + f(u, v), \quad \frac{\partial v}{\partial t} = g(u, v)$$

where $\varepsilon \ll 1$. The parameter ε is a dimensionless number which is the ratio of the rates of reaction of the quantities u and v . The diffusion coefficient is scaled by ε^2 because we take x on the doubly infinite real line, so space can be scaled freely.

The actual details of f and g are relatively unimportant except that they represent “typical” dynamics of excitable media such as the FitzHugh–Nagumo equation [6], [7], [21], [29]. In particular, we require the null cline $f(u, v) = 0$ to be “cubic-shaped” with $f(u, v) < 0$ for all v sufficiently large. The behavior of g is of little consequence to the derivation of the theory. However, to keep ideas specific, we assume that the curve $g(u, v) = 0$ is monotone having one intersection with the curve $f(u, v) = 0$ and that $g(u, v) > 0$ for u sufficiently large. This information is depicted in Fig. 1.

One important consequence of these assumptions on $f(u, v)$ is that the null cline $f(u, v) = 0$ has three solution branches, denoted $u = U_{\pm}(v)$ or $u = U_0(v)$ where $U_-(v) \leq U_0(v) \leq U_+(v)$ wherever comparison is appropriate. In fact, $U_-(v)$ exists only for $v > v_-$ and $U_+(v)$ exists only for $v < v_+$; it is essential that $v_+ > v_-$.

The system (2.1) for one-dimensional spatial domains can be treated using singular perturbation arguments [3], [5], [13]. These arguments reveal that a wave form consists

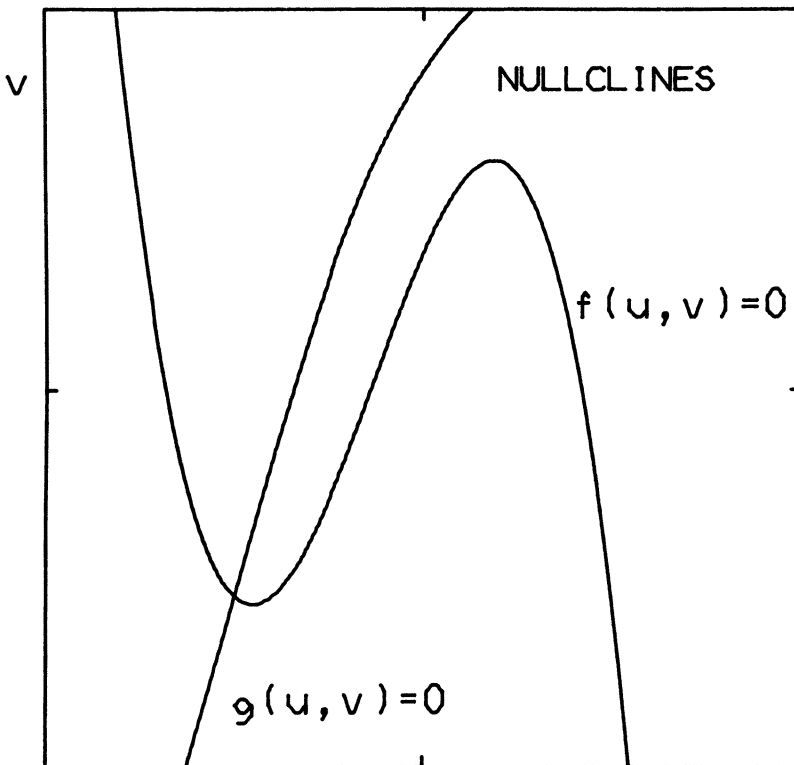


FIG. 1. Typical nullclines $f(u, v) = 0$ and $g(u, v) = 0$ for the excitable system (2.1).

of two typical regions. In the slowly varying region, diffusion has little effect, and u and v must satisfy, to lowest order in ε ,

$$(2.2) \quad \frac{\partial v}{\partial t} = g(u, v), \quad f(u, v) = 0.$$

This is obtained by setting $\varepsilon = 0$ in (2.1). For reasons of stability, equation (2.2) implies that either $u = U_+(v)$ or $u = U_-(v)$ and that on these solution branches, the slow dynamics are governed by

$$(2.3) \quad \frac{\partial v}{\partial t} = g(U_{\pm}(v), v) \equiv G_{\pm}(v).$$

The fact that u can lie on either the upper branch or lower branch of $f(u, v) = 0$ admits the possibility of spatial discontinuities in u . At such discontinuities diffusion becomes important, and regions corresponding to different solution branches of $f(u, v) = 0$ are patched together by a moving boundary layer. The boundary layer is found by making the change of variables $x = \varepsilon\xi + y(\tau)$, $t = \tau$, and seeking translation invariant solutions of the resulting equations (i.e., set $\partial/\partial\tau = 0$). To lowest order in ε , we obtain

$$(2.4) \quad \begin{aligned} Du'' + cu' + f(u, v_0) &= 0, & v_0 \text{ constant, } u &= u(\xi). \\ \lim_{\xi \rightarrow \pm\infty} f(u, v_0) &= 0, & c &= y'(\tau). \end{aligned}$$

In addition, the boundary layer must have the correct orientation, so that, for example, $\lim_{\xi \rightarrow \infty} u(\xi) = U_+(v_0)$ whenever the region immediately to the right of the boundary layer also has $u = U_+(v)$.

Although much more can be said about the use and interpretation of these equations, the behavior of waves in one-dimensional excitable media is captured nicely by the consistent application of equations (2.3) and (2.4).

The main consequence of this analysis for our theory is the specific equation (2.4). If we solve the nonlinear eigenvalue problem

$$(2.5) \quad \begin{aligned} Du'' + \mu u' + f(u, v_0) &= 0, \\ \lim_{\xi \rightarrow \infty} u(\xi) &= U_+(v_0), \\ \lim_{\xi \rightarrow -\infty} u(\xi) &= U_-(v_0), \end{aligned}$$

for D fixed, then the speed of propagation of the moving boundary layer is $c = \mu(v_0)$ if the boundary conditions have the same orientation, or $c = -\mu(v_0)$ if the opposite orientation applies.

For most problems the solution of the eigenvalue problem (2.5) must be carried out numerically. There are two cases where exact analytical solutions are known. In the special case that f is piecewise linear [21], [29], [38]

$$(2.6) \quad f(u, v) = H(u) - u - v$$

where $H(u)$ is the Heaviside step function, one can calculate directly that

$$(2.7) \quad \mu(v_0) = \frac{\sqrt{D}(1-2v_0)}{2\sqrt{v_0(1-v_0)}}.$$

In the cubic case

$$(2.8) \quad f(u, v) = -A(u - u_0)(u - u_1)(u - u_2)$$

where the roots satisfy $u_0 < u_1 < u_2$ and depend on v_0 , one can again calculate that

$$(2.9) \quad \mu(v_0) = \frac{\sqrt{DA}}{2}(u_0 - 2u_1 + u_2).$$

This follows if one makes the guess $u' = \alpha(u - u_0)(u - u_2)$ and substitutes into (2.5). It is useful to note that the sign of μ is determined by integrating the equation (2.5) to yield

$$(2.10) \quad \mu(v_0) \int_{-\infty}^{\infty} u'^2(\xi) d\xi = - \int_{U_-(v_0)}^{U_+(v_0)} f(y, v_0) dy.$$

In general, the speed of propagation of the moving boundary layers is not constant since in the medium ahead of the jump, the value of v_0 is changing in time. This complication makes solution of the full dynamic propagation problem difficult indeed. There are two special cases where wave speeds are constant. If the medium ahead of the jump is at rest, then the leading front travels at the speed determined by the constant value of v in the medium ahead. If there is a periodic wave train of up and down jumps, we also have constant propagation speeds, although this can occur if and only if the speed and period are chosen consistently. Suppose we seek solutions traveling with fronts corresponding to v value v_0 . Their speed is, naturally, $c = \mu(v_0)$, and the period must be consistent with the outer dynamics. Let v_1 be a v -value for which $\mu(v_1) = -\mu(v_0)$, or if no such value exists take $v_1 = v_+$ (phase waves), the local maximum of the null cline $f(u, v) = 0$. We take the down jump to have v value v_1 . Then from (2.2), the temporal period of the wave train must be $T = T(v_0)$ where

$$(2.11) \quad T(v_0) = \int_{v_0}^{v_1} \left(\frac{1}{g(u_+(v), v)} - \frac{1}{g(u_-(v), v)} \right) dv$$

to leading order in ε .

The relationship between $c(v_0)$ and $T(v_0)$ is, to first order in ε , the dispersion relation for the diffusion reaction system (2.1). Typically the c versus T curve is monotone increasing and bounded as $T \rightarrow \infty$, although by varying f and g one can easily arrange a wide assortment of dispersion curves, and associated solitary pulses and/or single transitions [5], [13].

For the specific example of piecewise linear dynamics (2.6) with

$$(2.12) \quad g(u, v) = u + \alpha, \quad 0 < \alpha < \frac{1}{2}$$

we find that

$$(2.13) \quad T(v_0) = \ln \left(\frac{(1 - v_0)^2 - \alpha^2}{v_0^2 - \alpha^2} \right),$$

which, coupled with (2.7), gives a parametric representation of the dispersion curve.

This representation of the dispersion curve becomes invalid as v_0 approaches v_0^* , where $\int_{U_-(v_0^*)}^{U_+(v_0^*)} f(u, v_0^*) du = 0$. (The value v_0^* corresponds to zero speed.) For $\varepsilon \neq 0$ fixed, the dispersion curve is known to have two branches, the one just calculated, corresponding to stable wave propagation, and a second branch of slow unstable periodic waves. These two branches coalesce at a “knee” whose location depends upon ε .

Although we shall not use the slow branch of the dispersion curve, it is important to know where the knee occurs. To determine this branch, we introduce the stretched traveling coordinate $\xi = (x - ct)/\varepsilon$ for which equations (2.1) become

$$(2.14) \quad Du'' + cu' + f(u, v) = 0, \quad cv' + \varepsilon g(u, v) = 0.$$

Our next step is motivated by the observations that the validity of the fast branch fails when c and the variation in v become small. Thus, we take $c = \varepsilon^{1/2}\mu$ and (2.14) becomes

$$(2.15) \quad Du'' + f(u, v) = -\varepsilon^{1/2}\mu u', \quad \mu v' = -\varepsilon^{1/2}g(u, v)$$

for which we seek periodic solutions.

The obvious thing to do is to seek periodic solutions which are power series in $\varepsilon^{1/2}$, $u = u_0 + \varepsilon^{1/2}u_1 + \dots$, $v = v_0 + \varepsilon^{1/2}v_1 + \dots$ and $\mu = \mu_0 + \varepsilon^{1/2}\mu_1 + \dots$. With this ansatz, we obtain a hierarchy of equations

$$(2.16) \quad Du_0'' + f(u_0, v_0) = 0, \quad \mu_0 v_0' = 0,$$

and

$$(2.17) \quad \begin{aligned} Du_1'' + \frac{\partial f}{\partial u}(u_0, v_0)u_1 &= -\left(\mu_0 u_0' + \frac{\partial f}{\partial v}(u_0, v_0)v_1\right), \\ \mu_0 v_1' &= -g(u_0, v_0). \end{aligned}$$

The solution of (2.16) is straightforward. We take $v_0 = \text{constant}$ and then find a periodic solution of $Du_0'' + f(u_0, v_0) = 0$. Since this is a Hamiltonian system which possesses a continuous family of periodic solutions for each fixed v_0 , at this point we have too many solutions.

Proceeding to the next order, we require

$$\mu_0 v_1' = -g(u_0, v_0).$$

Naturally v_1 must be periodic so we require

$$(2.18) \quad \int_0^P g(u_0(x), v_0) dx = 0,$$

where P is the period of the chosen solution $u_0(x)$. This condition enables us to select the correct periodic solution from among the family of periodic solutions of $Du_0'' + f(u_0, v_0) = 0$. We denote the period of this correctly chosen solution as $P(v_0)$. With this periodic solution $u_0(x)$ selected, the solution of (2.17) becomes possible only if the orthogonality condition

$$(2.19) \quad \int_0^P \left(\mu_0 u_0'^2 + \frac{\partial f}{\partial v}(u_0, v_0)v_1 u_0' \right) dx = 0$$

is satisfied.

Substituting the known solution for v_1 , we have

$$(2.20) \quad \mu_0^2 \int_0^P u_0'^2 dx = - \int_0^P u_0' \frac{\partial f}{\partial v}(u_0, v_0) \left[\int_0^x g(u_0, v_0) d\eta \right] dx$$

which uniquely determines $\mu_0(v_0)$. Re-expressing this information in the original coordinate system, we find that the wavelength, period and speed of the traveling

wavetrain are, to leading order in ε ,

$$(2.21) \quad \begin{aligned} \Lambda &= \varepsilon P(v_0), \\ T &= \frac{\varepsilon^{1/2} P(v_0)}{\mu_0(v_0)}, \\ c &= \varepsilon^{1/2} \mu_0(v_0), \end{aligned}$$

parametrized by v_0 . The form of the expressions (2.21) will be important to us later.

As a specific example, we can calculate this branch of the dispersion curve explicitly for the piecewise linear FitzHugh–Nagumo dynamics (2.6), (2.12). With these choices of f and g , equation (2.20) becomes

$$\mu_0^2 \int_0^P u_0'^2 dx = \int_0^P u_0^2 dx$$

which can be evaluated directly using hyperbolic trigonometric functions. In Fig. 2, we plot the two branches of the dispersion curve for the piecewise linear FitzHugh–Nagumo equations in the speed-frequency coordinate system, where frequency is $\omega = 2\pi/T$, for $\alpha = .1$, $\varepsilon = .1$ and $\varepsilon = .05$. These approximate results agree quite well with the exact results published in [29].

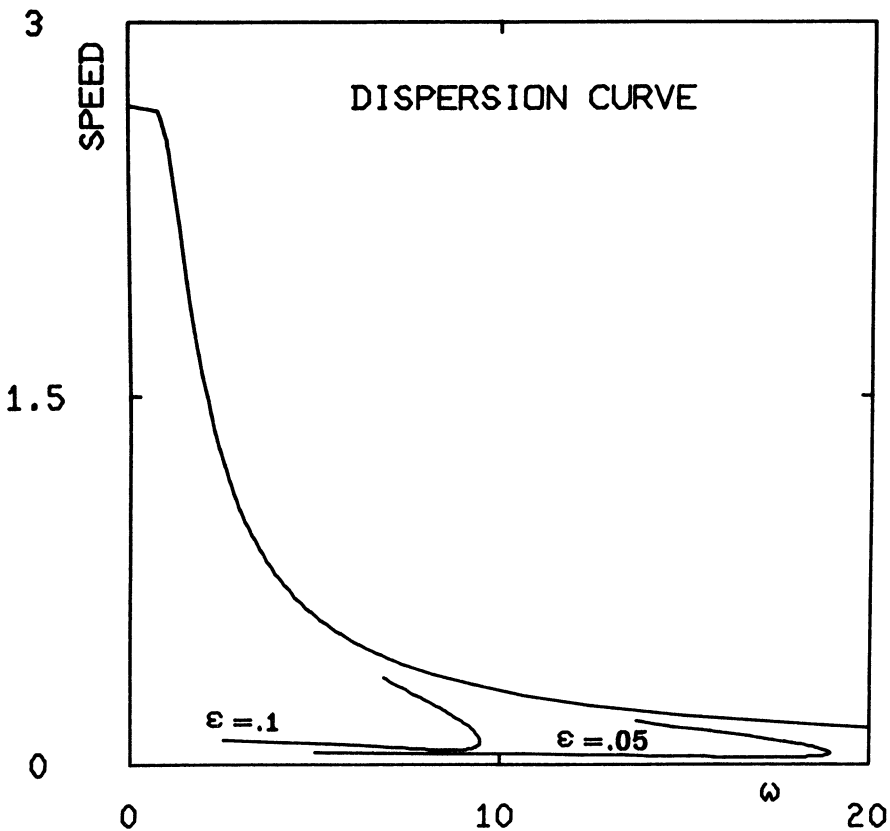


FIG. 2. Dispersion curve speed vs. ω for piecewise linear FitzHugh–Nagumo equation with $\alpha = .1$, $\varepsilon = .1$ and $\varepsilon = .05$.

3. Derivation of the eikonal equation. We want to extend the theory of moving boundary layers in one space dimension to waves in media with higher spatial dimension. To find a boundary layer in \mathbb{R}^2 , we introduce a stretched traveling coordinate system

$$(3.1) \quad x = X(\varepsilon\xi, \eta, \tau), \quad y = Y(\varepsilon\xi, \eta, \tau), \quad t = \tau$$

where ξ and η are locally orthogonal coordinates. The reason for this particular choice is that we seek translation invariant solutions with η as the wavefront coordinate. That is, we seek solutions for which the curves $\xi = \text{constant}$ are level curves of u , and the wavefront motion is depicted entirely by the movement of the coordinate system.

In this new coordinate system, partial derivatives take the form

$$(3.2) \quad \begin{aligned} \frac{\partial u}{\partial t} &= \frac{1}{\sqrt{(X_1^2 + Y_1^2)(X_2^2 + Y_2^2)}} \left\{ \frac{1}{\varepsilon} (X_2 Y_3 - Y_2 X_3) \frac{\partial u}{\partial \xi} + (X_3 Y_1 - Y_3 X_1) \frac{\partial u}{\partial \eta} \right\} + \frac{\partial u}{\partial \tau}, \\ \nabla^2 u &= \frac{1}{\varepsilon^2} \frac{1}{\sqrt{X_1^2 + Y_1^2}} \left\{ \frac{\partial}{\partial \xi} \left(\frac{1}{\sqrt{X_1^2 + Y_1^2}} \frac{\partial u}{\partial \xi} \right) + \varepsilon K_2 \frac{\partial u}{\partial \xi} \right\} \\ &\quad + \frac{1}{\sqrt{X_2^2 + Y_2^2}} \left\{ \frac{\partial}{\partial \eta} \left(\frac{1}{\sqrt{X_2^2 + Y_2^2}} \frac{\partial u}{\partial \eta} \right) - K_1 \frac{\partial u}{\partial \eta} \right\} \end{aligned}$$

where X_i, Y_i represent partial derivatives with respect to their i th argument, and K_1, K_2 are curvatures

$$(3.3) \quad K_i = \frac{X_i Y_{ii} - Y_i X_{ii}}{(X_i^2 + Y_i^2)^{3/2}}.$$

The orientation for the ξ - η coordinate axes is the same as the usual x - y axes, that is, the positive ξ axis is rotated 90 degrees in the clockwise direction from the positive η axis.

Without loss of generality, we take $X_1^2 + Y_1^2 = 1$ and seek solutions with $\partial u / \partial \eta = \partial u / \partial \tau = 0$. With these assumptions and restrictions, we find that (2.1) becomes

$$(3.4) \quad \begin{aligned} \text{i) } D \frac{\partial^2 u}{\partial \xi^2} + (N_2 + \varepsilon D K_2) \frac{\partial u}{\partial \xi} + f(u, v) &= 0, \\ \text{ii) } N_2 \frac{\partial v}{\partial \xi} &= \frac{\varepsilon N_1}{(X_2^2 + Y_2^2)^{1/2}} \frac{\partial v}{\partial \eta} + \varepsilon \frac{\partial v}{\partial \tau} + \varepsilon g(u, v) \end{aligned}$$

where $N_i = (X_3 Y_i - Y_3 X_i) / (X_i^2 + Y_i^2)^{1/2}$, $i = 1, 2$, is the normal velocity of the coordinate lines.

From equation (3.4ii) we learn that $v = v_0 + O(\varepsilon)$. If N_2 and K_2 were independent of ξ , we could identify equation (3.4i) with (2.5) and require

$$(3.5) \quad N_2 + \varepsilon D K_2 = \mu(v_0).$$

Fortunately, the ξ variation does not affect this approximation significantly. To see this, we represent the coordinate system locally by

$$(3.6) \quad \begin{aligned} X(\xi, \eta, \tau) &= X_0(\eta, \tau) + \frac{\xi X_{0\eta}}{(X_{0\eta}^2 + Y_{0\eta}^2)^{1/2}} + O(\xi^2), \\ Y(\xi, \eta, \tau) &= Y_0(\eta, \tau) + \frac{\xi Y_{0\eta}}{(X_{0\eta}^2 + Y_{0\eta}^2)^{1/2}} + O(\xi^2). \end{aligned}$$

Then, by a direct, but tedious, calculation, it follows that $N_2 = N_2|_{\xi=0} + O(\xi^2)$. Thus, to order ε^2 , $N_2 + \varepsilon D K_2$ is independent of ξ , justifying the identification (3.5).

As a result

$$N_2 + \varepsilon DK_2 = \mu(v_0) + O(\varepsilon).$$

One might argue that keeping the curvature correction term εDK_2 makes no difference to this order of approximation. However, as we shall see, K_2 need not be independent of ε and in fact, must be retained for spirals since there $K_2 = O(\varepsilon^{-2/3})$. The extra work needed to get the curvature correction in equation (3.5) is further justified by the fact that the easier approximation $N = \mu(v_0)$ fails miserably when applied to spiral structures.

In general, the value of v_0 may change with the spatial and temporal position of the wave front unless we restrict our attention to solitary or periodic waves. In this case we have

$$(3.7) \quad N = \mu(T) - \varepsilon DK$$

where $\mu(T)$ denotes the dispersion relation for wave speed as a function of period $T = T(v_0)$, specified by (2.11), and where

$$N = \frac{X_\tau Y_\eta - Y_\tau X_\eta}{(X_\eta^2 + Y_\eta^2)^{1/2}}, \quad K = \frac{X_\eta Y_{\eta\eta} - Y_\eta X_{\eta\eta}}{(X_\eta^2 + Y_\eta^2)^{3/2}}$$

are the normal velocity and curvature, respectively, of the wave front at $\xi = 0$.

The equation (3.7) has a very nice geometrical interpretation. Since $\mu(T)$ is the velocity of plane waves of period T , (3.6) implies that $\mu(T)$ is the velocity of plane waves of period T , and the normal velocity is decreased by curvature away from the direction of forward propagation and enhanced by curvature toward the direction of forward propagation with an influence having the same order of magnitude as the diffusion coefficient εD . Note also that the term εDK has dimensional units of velocity. These observations make good physical sense. For example, a point just ahead of a front with curvature in the direction of motion will be more quickly excited to threshold than if it were approached by a plane wave, since curvature tends to focus the stimuli necessary to excite the point. The equation (3.7) has been used in studies of flame front propagation [19] and crystal growth [31]. The fact that curvature influences the velocity of waves in excitable media was previously noted in [40], [41].

The equation (3.7) is related to the eikonal equation of geometrical optics. In optics, the eikonal equation is $N = \mu$, where μ depends only on space, and not on the period of the waves. Furthermore, there is no curvature effect on the speed of wave fronts. The approximation $N = \mu$ was used in [9] for excitable media problems.

In optics there are two standard ways to derive the eikonal equation. One may assume that waves have high frequency, or that solutions are discontinuous along the wavefront [34]. The second of these assumptions is analogous to our problem since we have assumed that transitions between the two possible states of the medium are sharp.

The equation (3.7) is the basis of our geometrical theory. We can express this equation in a way that suggests propagation along "rays". Suppose the wavefront at $\xi = 0$ is given by $x = X(\eta, \tau)$, $y = Y(\eta, \tau)$ and satisfies $X_\tau X_\eta + Y_\tau Y_\eta = 0$ (i.e., the τ -tangent vector and η -tangent vector are orthogonal), then (3.7) can be rearranged into

$$(3.8) \quad \begin{aligned} X_\tau &= \left\{ \mu(T) - \varepsilon D \frac{X_\eta Y_{\eta\eta} - Y_\eta X_{\eta\eta}}{(X_\eta^2 + Y_\eta^2)^{3/2}} \right\} \frac{Y_\eta}{(X_\eta^2 + Y_\eta^2)^{1/2}}, \\ Y_\tau &= - \left\{ \mu(T) - \varepsilon D \frac{X_\eta Y_{\eta\eta} - Y_\eta X_{\eta\eta}}{(X_\eta^2 + Y_\eta^2)^{3/2}} \right\} \frac{X_\eta}{(X_\eta^2 + Y_\eta^2)^{1/2}}. \end{aligned}$$

In this form, we see that the “eikonal” equation is parabolic and that neighboring “rays” interact through an order ε diffusion term. These equations represent a noticeable simplification of (2.1). In (3.8) we have a coupled system of nonlinear parabolic equations in the one space variable η and two state variables X , Y , whereas (2.1) is a system of parabolic equations in 2 space variables x and y and the two state variables u and v with stiff, relaxation dynamics.

4. Rotating spiral waves. Spiral patterns in excitable media occur in a wide variety of situations. For example, rotating waves have been observed in BZ reagent [1], [36], [39], in heart muscle [2], [24], [4], in rat cortex [30], and in the retina of the eye [20]. Much of the analytical work on spiral patterns has been restricted to self-oscillatory media, especially of $\lambda - \omega$ type. In this section we discuss the application of our geometrical theory to excitable problems in polar geometry.

We begin by looking for k -armed spiral wavefronts of the form

$$(4.1) \quad \begin{aligned} X_j &= r \cos \left(\theta(r) - \omega t + \frac{2\pi j}{k} \right), \quad j = 1, 2, \dots, k, \\ Y_j &= r \sin \left(\theta(r) - \omega t + \frac{2\pi j}{k} \right) \end{aligned}$$

where for geometrical reasons we expect $\theta' \omega > 0$. (Here the wavefront coordinate η is the radial variable r .) Our goal is to find solutions of (3.7) on an annulus $r_0 \leq r \leq r_1$, with the aim of letting r_0 approach zero. As boundary conditions, we require $\theta'(r_0) = 0$ and $\theta'(r_1) = 0$ which imply that the spiral arms are orthogonal to the circular boundaries, equivalent to no-flux conditions at the boundaries. If $r_1 = \infty$, we want $\theta(r)$ to be asymptotically linear so that (4.1) is asymptotically Archimedean. If we specify the periodicity T of the solutions, then for consistency we must have

$$(4.2) \quad \omega = \frac{2\pi}{kT}.$$

From (4.1) we directly calculate the normal velocity and curvature as

$$(4.3) \quad N = \frac{\omega r}{(1 + \psi^2)^{1/2}}, \quad K = \frac{\psi'}{(1 + \psi^2)^{3/2}} + \frac{\psi}{r(1 + \psi^2)^{1/2}},$$

where $\psi = r\theta'(r)$.

Before solving (3.7), it is instructive to solve the zeroth order eikonal equation $N = \mu(T)$. By simple quadrature we find that

$$(4.4) \quad \theta(r) = \left(\frac{r^2}{r_0^2} - 1 \right)^{1/2} - \tan^{-1} \left(\frac{r^2}{r_0^2} - 1 \right)^{1/2}, \quad r_0 = \frac{\mu}{\omega}.$$

With the change of variables $s = ((r^2/r_0^2) - 1)^{1/2}$ we obtain wavefronts of the form

$$(4.5) \quad \begin{aligned} X(s) &= r_0 \cos s + r_0 s \sin s, \\ Y(s) &= r_0 \sin s - r_0 s \cos s \end{aligned}$$

which is the parametric representation of the involute of a circle of radius r_0 . In other words, the involute of a circle solves $N = \mu$. The geometrical similarity of spirals to involutes is noted in [36].

There are some significant difficulties with the involute solution. First, for consistency, we must choose $r_0 = \mu(T)T/2\pi$, but for small r_0 this may not be possible since the dispersion curve $\mu(T)$ has a knee. Even if there is no knee, an involute

becomes degenerate as r_0 approaches zero. Thus, this solution fails if the central core is too small. Second, for any value of r_0 , near the circle of radius r_0 , the curvature of the involute is arbitrarily large so that curvature effects must be important, and the involute solution cannot be valid there. Finally, the boundary condition at r_1 cannot be satisfied unless $r_1 = \infty$. All of these defects are corrected by the higher order theory (3.7).

To solve (3.7), we require

$$(4.6) \quad r \frac{d\psi}{dr} = (1 + \psi^2) \left(\frac{r\mu}{\varepsilon} (1 + \psi^2)^{1/2} - \frac{\omega r^2}{\varepsilon} - \psi \right), \quad \psi = r\theta'(r).$$

(Without loss of generality, we now take $D = 1$.) A typical phase portrait for (4.6) is shown in Fig. 3a. The only critical point is a saddle point at $r = \psi = 0$. For values of μ/ε large, the equation is quite stiff with a unique, strongly attracting trajectory. Trajectories for three different values of ω/ε with $\mu/\varepsilon = 3$ and $r_1 = 9$ fixed are shown in Fig. 3b.

We view the equation (4.6) as an eigenvalue problem, and wish to find the parameter values μ/ε and ω/ε for which trajectories connect the points $\psi = 0$ at $r = r_0$ with $\psi = 0$ at $r = r_1$. Notice that the vector field of (4.6) is monotone increasing in μ/ε and decreasing in ω/ε . Therefore for any fixed r_0, r_1 (including $r_0 = 0$), there are values of ω, μ for which trajectories of (4.6) connect $\psi = 0, r = r_0$ with $\psi = 0, r = r_1$. We can

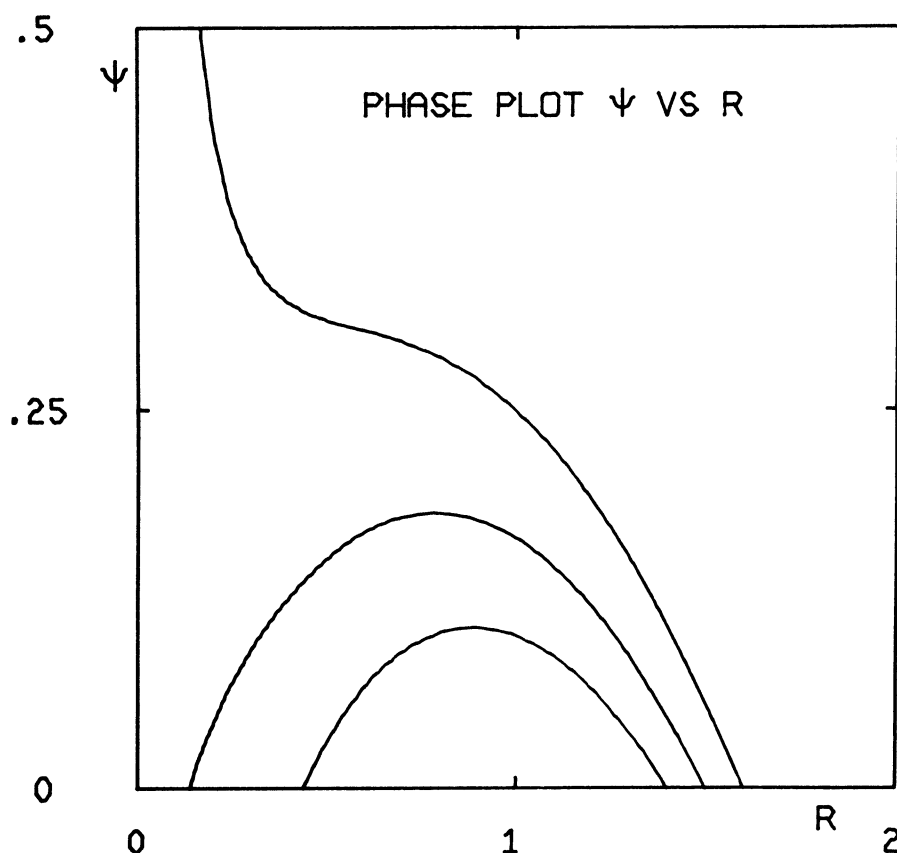


FIG. 3a. Phase plot for equation (4.6) with $\omega/\varepsilon = 1$, $\mu/\varepsilon = 1$. Trajectories shown for $r_1 = 1.4, 1.5$ and 1.6 .

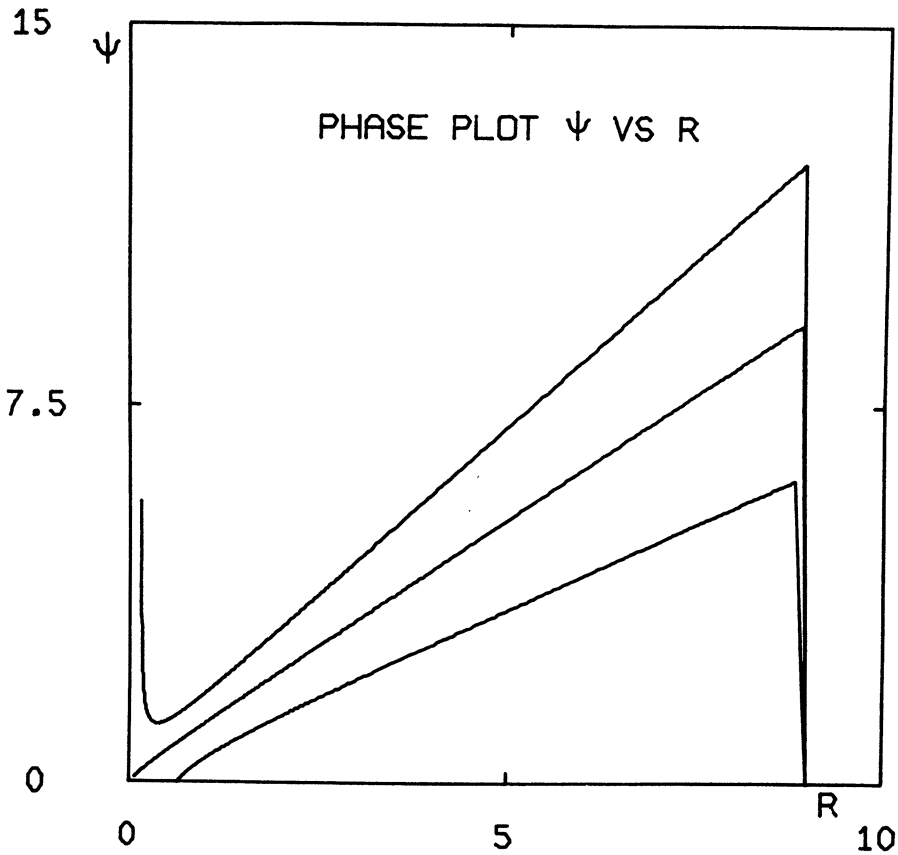


FIG. 3b. Trajectories for (4.6) with $r_1 = 9$, $\mu/\varepsilon = 3$ and $\omega/\varepsilon = 2.8, 9m^*$ and 3.2.

represent this relationship as

$$(4.7) \quad \frac{\omega}{\varepsilon} = \Omega\left(\frac{\mu}{\varepsilon}, r_0, r_1\right)$$

where Ω is monotone increasing in μ , and monotone decreasing in r_0 and r_1 . The function Ω is invariant under a change of scale. The change of variables $r \rightarrow \alpha r$, $\mu \rightarrow \mu/\alpha$ and $\omega \rightarrow \omega/\alpha^2$ leaves the equation (4.6) invariant, so for any scalar α

$$(4.8) \quad \omega = \varepsilon \alpha^2 \Omega\left(\frac{\mu}{\varepsilon \alpha}, \alpha r_0, \alpha r_1\right),$$

or, if we pick $\alpha = 1/r_1$,

$$(4.9) \quad \omega = \frac{\varepsilon}{r_1^2} \Omega\left(\frac{r_1 \mu}{\varepsilon}, \frac{r_0}{r_1}, 1\right)$$

where the third argument is equal to one and no longer noted. Because the equation (4.6) is stiff, (4.7) is independent of r_1 for r_1 large.

Using perturbation arguments, we can show that

$$(4.10) \quad \Omega(x, y) = \frac{3x(y+1)}{2y^2 + y + 1} + O(x^3)$$

and that

$$(4.11) \quad \Omega(x, 0) = \frac{3x}{2} + \frac{3}{560}x^3 + \frac{331}{3449600}x^5 + O(x^7).$$

Numerically, we have determined that for $x \geq 10$, Ω is accurately represented by

$$(4.12) \quad \Omega(x, y) = m^*x^2 - \alpha x^4 y^2 + O(y^4)$$

where $m^* = 0.330958$, $\alpha = .097$.

The solution of our problem can be achieved graphically by finding the intersection of the two curves

$$(4.13) \quad \mu = \mu\left(\frac{2\pi}{k\omega}\right), \quad \omega = \frac{\varepsilon}{r_1^2} \Omega\left(\frac{r_1 \mu}{\varepsilon}, \frac{r_0}{r_1}\right).$$

In Fig. 4, we plot these two curves in the $\mu - \omega$ parameter space for $r_0 = 0$. For purposes of illustration we use the specific dispersion curve (2.7), (2.13) for the piecewise linear dynamics (2.6), (2.12) with $\alpha = .1$ and $\varepsilon = .1$ and $\varepsilon = .05$. The intersection of these curves specifies the frequency ω and asymptotic speed μ for a spiral with inner radius r_0 . Since this intersection depends in general on the inner core size r_0 , in Fig. 5 is plotted the inner core size r_0 as a function of ω as the intersection moves along the dispersion curve and in Fig. 6 is plotted the asymptotic speed μ as a function of

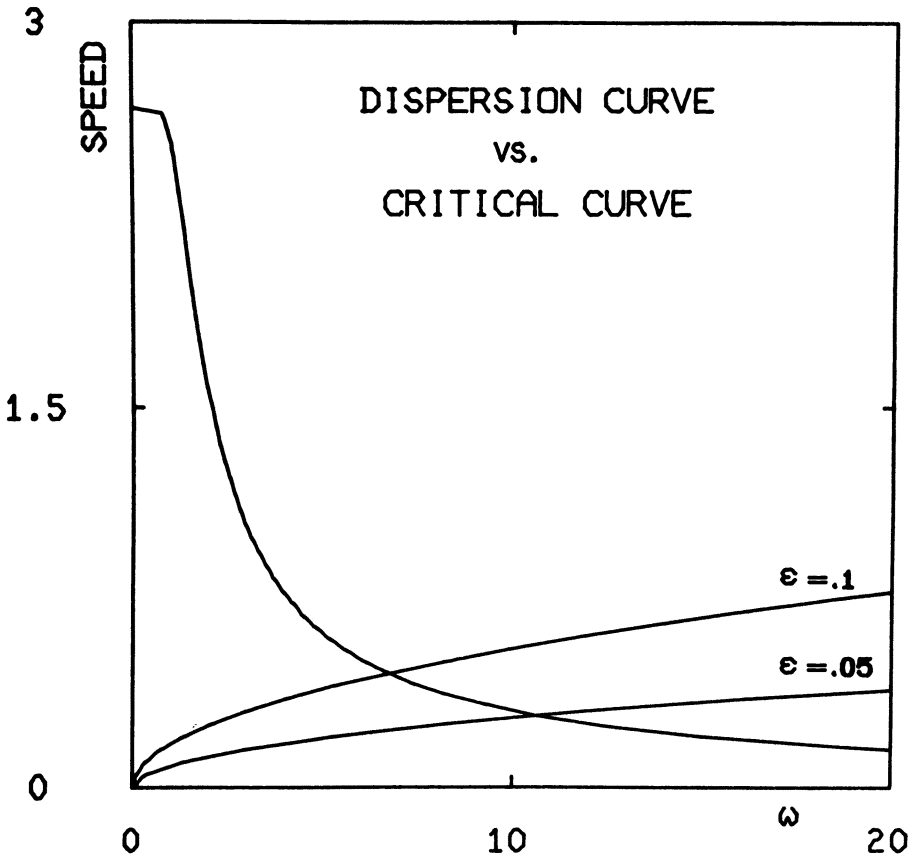


FIG. 4. Plot of dispersion curve and critical curve (4.9) for $r_1 = 10$, $r_0 = 0$ with $\alpha = .1$, $\varepsilon = .1, .05$.

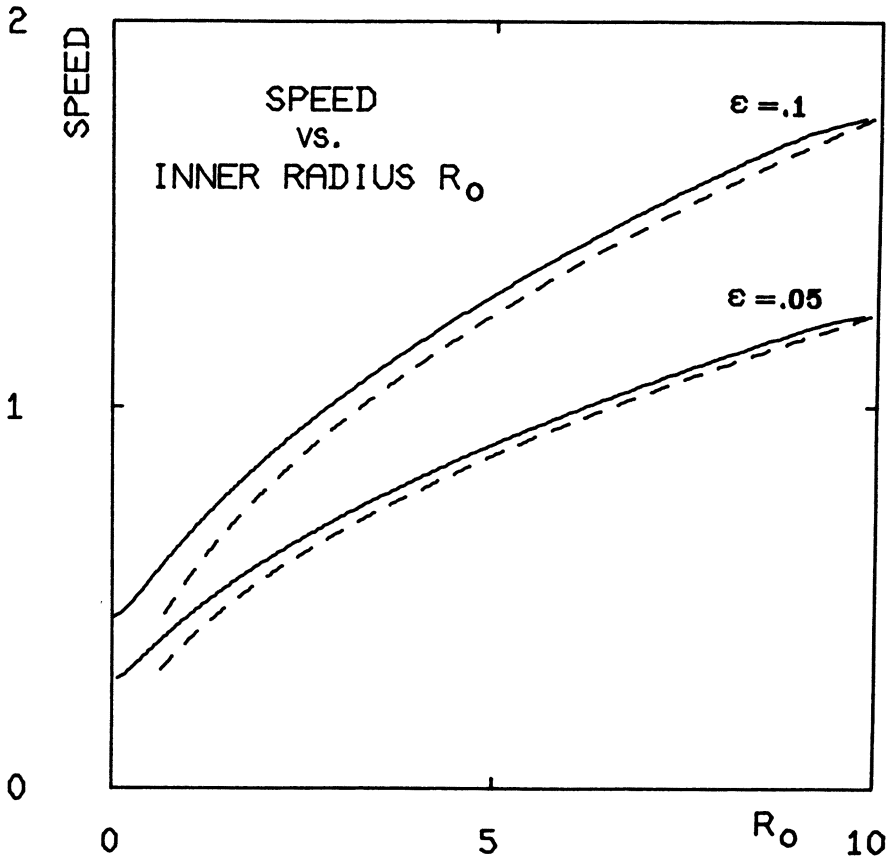


FIG. 5. Plot of inner radius r_0 as a function of ω along the dispersion curve with $\alpha = .1$, $r_1 = 10$ for solution of (4.6) (solid curve) and for an involute (dashed curve) for $\epsilon = .1, .05$.

inner core size r_0 moving along the dispersion curve. The dashed curve in these figures corresponds to taking $r_0 = \mu(T)/\omega$ which one obtains using involutes. The important thing to notice is that ω and μ are now determined for any core size, even $r_0 = 0$, whereas the involute fails for small r_0 . In these plots we have taken $r_1 = 10$, although the results are insensitive to r_1 .

We can give analytical estimates of ω and μ for small ϵ for r_0 small. For $r_0 = 0$, the parameter curve (4.19) is approximated by

$$(4.14) \quad \omega = \frac{\mu^2 m^*}{\epsilon}$$

independent of r_1 . We approximate the dispersion curve $\mu = \mu(2\pi/k\omega)$ by

$$(4.15) \quad \mu \sim \frac{C}{k\omega}$$

where

$$C = \pi \left| \frac{c'(v^*) G_+(v^*) G_-(v^*)}{G_+(v^*) - G_-(v^*)} \right|,$$

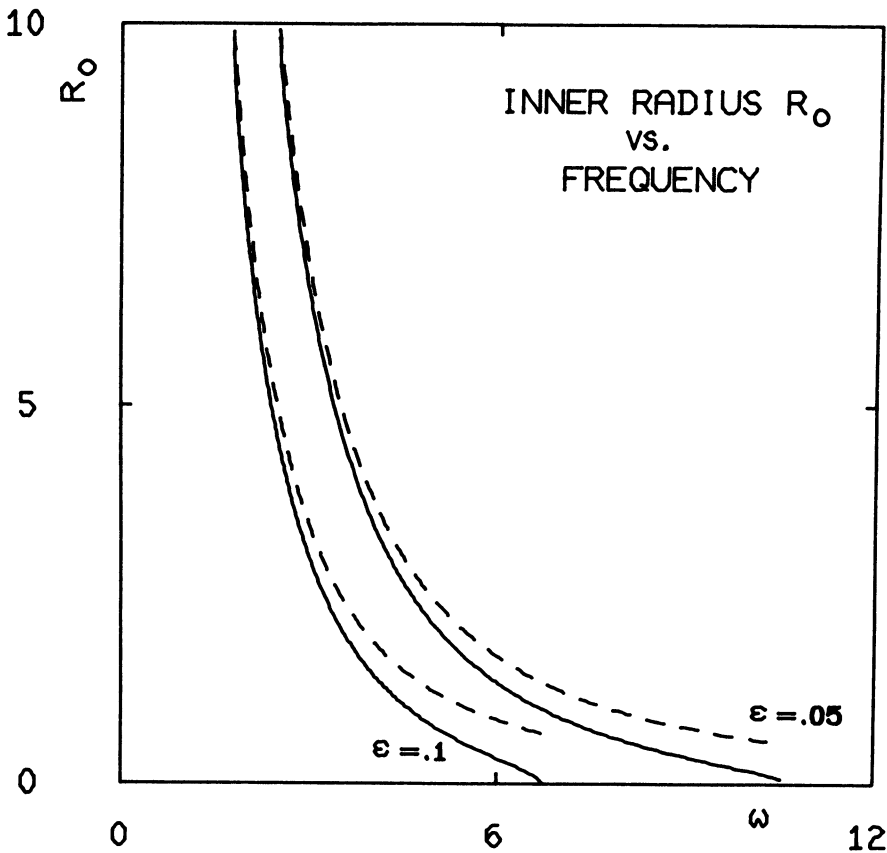


FIG. 6. Plot of wave speed as a function of inner radius r_0 along the dispersion curve with $\alpha = .1$, $r_1 = 10$ for solution of (4.6) (solid curve), and for an involute (dashed curve) for $\varepsilon = .1, .05$.

$c(v)$ is the eigenvalue of equation (2.4), and $c(v^*) = 0$. This relationship approximates the dispersion curve for large frequencies ω provided ω is not so large as to be near the knee of the dispersion curve. For the piecewise linear FitzHugh–Nagumo dynamics (2.6), (2.12)

$$(4.16) \quad C = 2\pi\left(\frac{1}{4} - \alpha^2\right).$$

Using these estimates, we find that the intersection of the curves (4.14) and (4.15) occurs at

$$(4.17) \quad \omega = \left(\frac{C^2 m^*}{k^2 \varepsilon}\right)^{1/3}, \quad \mu = \left(\frac{C \varepsilon}{k m^*}\right)^{1/3}.$$

The intersection of the curves (4.14) and (4.15) does not occur near the knee of the dispersion curve. To see this, note that according to (2.21) the knee of the dispersion curve has frequency of order $\varepsilon^{-1/2}$, while here we find that ω is of order $\varepsilon^{-1/3}$. It follows that for small enough ε the frequency of the spiral is not determined by the location of the knee of the dispersion curve. The knee of the dispersion curve predicts frequencies which are too large and speeds which are too small.

The spiral trajectories we find here are Archimedean spirals in the limit $r \rightarrow \infty$. They differ from involutes only in the neighborhood of the origin. The shape of all

spirals with $r_0 = 0$ and r_1 large is the same. For r_1 large and $r_0 = 0$ we can write (4.7) as

$$(4.18) \quad \begin{aligned} \frac{d\psi}{ds} &= -(1 + \psi^2)(\rho(1 + \psi^2)^{1/2} - m^* \rho^2 - \psi), \\ \frac{d\rho}{ds} &= -\rho, \\ \frac{d\theta}{ds} &= -\psi \end{aligned}$$

where the radial variable is $r = (\varepsilon/\mu)\rho(s)$. Thus, the spiral wavefronts (4.1) take the form

$$\begin{aligned} X_j(s, t) &= \frac{\varepsilon}{\mu} \rho(s) \cos \left(\theta(s) - \omega t + \frac{2\pi j}{k} \right), \\ Y_j(s, t) &= \frac{\varepsilon}{\mu} \rho(s) \sin \left(\theta(s) - \omega t + \frac{2\pi j}{k} \right), \end{aligned} \quad j = 1, 2, \dots, k,$$

where $\rho(s)$, $\theta(s)$ are independent of all parameters of the problem. Of course, the scale factor ε/μ and rotation speed ω are determined by the dispersion curve and the critical curve $\omega = m^* \mu^2/\varepsilon$. In Fig. 7 we compare the solution of (4.18) (solid curve) with an involute with the same asymptotic wavelength.

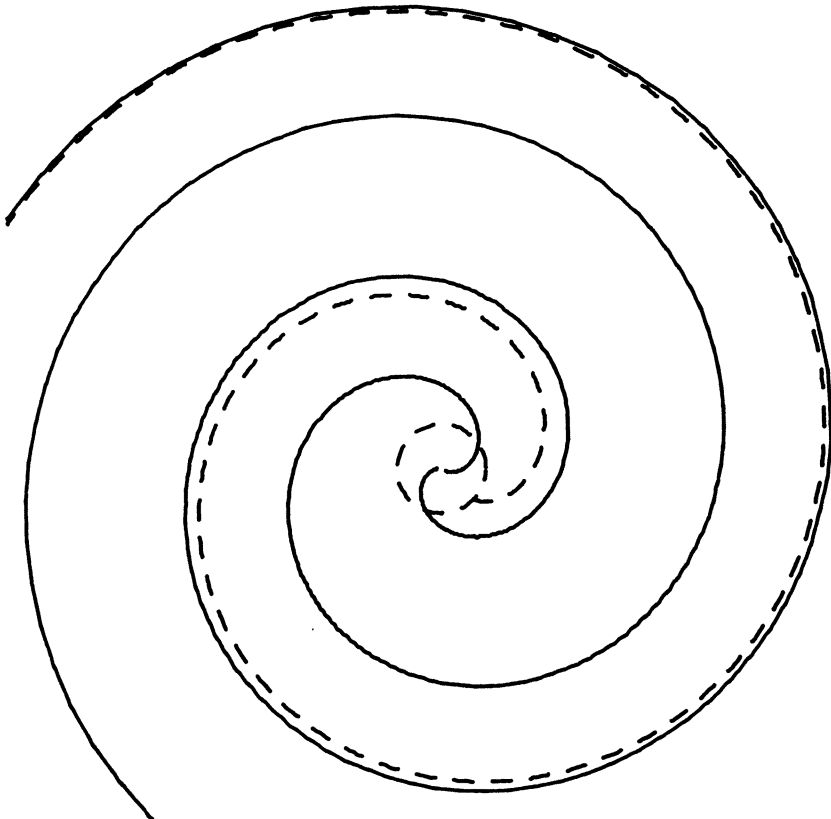


FIG. 7. Plot of spiral wavefront for (4.6) (solid curve) and for involute (dashed curve) at the intersection of dispersion curve with critical curve (see Fig. 4) $\omega/\varepsilon = 6.7172$, $\mu/\varepsilon = 4.511$ with $r_1 = 10$, $\varepsilon = .1$.

Although the core size r_0 for a fixed frequency is uniquely determined by (4.13), the reverse is not necessarily true. If the dispersion curve $\mu = \mu(T)$ is not monotone, then the inner core size r_0 need not be a monotone function of ω . In this situation an experiment which varies core size and determines the frequency ω would observe a hysteresis. A numerical simulation [27] on a modification of the FitzHugh–Nagumo equations produced such a hysteresis.

This approximate theory predicts a unique wavelength and period for a rotating spiral. However, because of the approximate analysis, the wave fronts cannot be expected to be accurate very close to the center of the spiral. This is because the boundary layer wavefront has a “thickness” of order ε , but near the center there is not enough room for such a boundary layer. One expects this approximation to become invalid for inner core size of order ε .

Even though the wavefronts are not valid near the center, the wavespeed and frequency of the spiral do not change much for small core size r_0 of order ε . This can be seen by estimating the behavior of the solution as a function of inner core size r_0 . Using (4.12) and (4.14), we find that for $r_0 \ll \varepsilon^{2/3}$,

$$(4.19) \quad \begin{aligned} \mu &= \left(\frac{C\varepsilon}{km^*} \right)^{1/3} \left(1 + \frac{\alpha}{3m^*} \left(\frac{C}{m^*k\varepsilon^2} \right)^{2/3} r_0^2 + \cdots \right), \\ \omega &= \left(\frac{C^2 m^*}{k^2 \varepsilon} \right)^{1/3} \left(1 - \frac{\alpha}{3m^*} \left(\frac{C}{m^*k\varepsilon^2} \right)^{2/3} r_0^2 + \cdots \right) \end{aligned}$$

which is quadratic in r_0 . The quadratic dependence of μ and ω on r_0 can also be seen visually in Figs. 5 and 6.

5. Discussion. A geometrical theory for wave fronts in excitable media has been derived using singular perturbation arguments. This theory is similar to geometrical optics in that wave fronts are shock like, and the wave front equation can be interpreted as a generalization of the eikonal equation. Using this theory we have found spiral patterns on a disc. Other important geometries can also be studied.

One limitation of this theory is that there are excitable systems which do not have relaxation type dynamics. However, for a wide range of physically important systems, such as the BZ reagent and myocardium, relaxation dynamics provide a reliable approximation to the truth.

This theory can and should be compared with numerical and experimental results. In this paper we have applied our techniques to the specific example of piecewise linear FitzHugh–Nagumo dynamics (2.6), (2.11) to get not only qualitative but quantitative predictions on frequency and wavelength of spirals. Unfortunately, accurate numerical solutions of equations (2.1) with ε small are quite difficult to obtain. In a forthcoming paper [14], the equivalent results for the Oregonator equations will be compared with experimental results for BZ reagent.

A possible extension of this theory is to use (3.7) in a kinematic way, with the correct dispersion relation, without reference to the smallness of ε . How valid such an approach will be is not yet known. However, using kinematics in one spatial dimension, Rinzel and coworkers [23], [28] have been quite successful in studying the dynamics of more complicated periodic structures without assuming relaxation type dynamics.

An alternate geometric approach for spiral solutions is suggested in [10], and partially exploited in [17], [22]. This theory applies to systems of diffusion reaction equations with equal diffusion coefficients with a known dispersion relation governing the speed and frequency of periodic traveling waves. The theory does not require

different time scales, is valid in the long wave limit and requires a complete knowledge of the dispersion relation. The resulting phase plane trajectories for spirals depend in a strongly nonlinear way on the dispersion relation, which complicates significantly full analysis of the problem.

In [22] an attempt is made to allow unequal diffusion coefficients and to exploit the smallness of ϵ . However a significant problem results from the unorthodox way that the dispersion relationship is defined and used. The phase plane analysis that results is, in principle, the same as ours, but is more difficult to decipher. With the results of [22], analytical solutions for the piecewise linear FitzHugh–Nagumo equations are possible only in a restricted parameter range.

Acknowledgments. The author gratefully acknowledges the hospitality of the Centre for Mathematical Biology at Oxford University and its director, J. D. Murray where this work was initiated, and discussions with J. J. Tyson, J. Rinzel and C. Peskin which were invaluable.

REFERENCES

- [1] K. I. AGLADZE AND V. I. KRINSKY, *Multi-armed vortices in an active chemical medium*, *Nature*, 296 (1982), pp. 424–426.
- [2] M. A. ALLESSIE, F. I. M. BONKE AND F. J. G. SCHOPMAN, *Circus movement in rabbit atrial muscle as a mechanism of tachycardia*, *Circ. Res.*, 41 (1977), pp. 9–18.
- [3] R. G. CASTEN, H. COHEN AND P. A. LAGERSTROM, *Perturbation analysis of an approximation to the Hodgkin–Huxley theory*, *Quart. Appl. Math.*, 32 (1975), pp. 365–402.
- [4] N. EL-SHERIF, R. MEHRA, W. B. GOUGH AND R. H. ZEILER, *Ventricular activation patterns of spontaneous and induced ventricular rhythms in canine one-day-old myocardial infarction*, *Circ. Res.*, 51 (1982), pp. 152–166.
- [5] P. C. FIFE, *Singular perturbation and wave front techniques in reaction-diffusion problems*, *Proc. AMS-SIAM Symp. on Asymptotic Methods and Singular Perturbation*, New York, 1976.
- [6] R. FITZHUGH, *Impulse and physiological states in models of nerve membrane*, *Biophysics J.*, 1 (1961), pp. 445–466.
- [7] ———, *Mathematical models of excitation and propagation in nerve*, in *Biological Engineering*, H. P. Schwan, ed., McGraw-Hill, New York, 1969, pp. 1–85.
- [8] K. O. FRIEDRICHS AND J. B. KELLER, *Geometrical acoustics II: Diffraction, reflection and refraction of a weak spherical or cylindrical shock at a plane interface*, *J. Appl. Phys.*, 26, 8 (1955), pp. 961–966.
- [9] B. C. GOODWIN AND M. H. COHEN, *A phase-shift model for the spatial and temporal organization of developing systems*, *J. Theoret. Biol.*, 25 (1969), pp. 49–107.
- [10] J. M. GREENBERG, *Periodic solutions to reaction-diffusion equation*, *this Journal*, 30 (1976), pp. 199–205.
- [11] J. M. GREENBERG AND S. P. HASTINGS, *Spatial patterns for discrete models of diffusion in excitable media*, *this Journal*, 34 (1978), pp. 515–523.
- [12] A. L. HODGKIN AND A. F. HUXLEY, *A quantitative description of membrane current and its application to conduction and excitation in nerve*, *J. Physics (London)*, 117 (1952), pp. 500–544.
- [13] J. P. KEENER, *Waves in excitable media*, *this Journal*, 39 (1980), pp. 528–548.
- [14] J. P. KEENER AND J. J. TYSON, *Spiral waves in the Belousov–Zhabotinskii reaction*, to appear.
- [15] J. B. KELLER, *Geometrical acoustics I, The theory of weak shocks*, *J. Appl. Phys.*, 25 (1954), pp. 1938–1947.
- [16] ———, *A geometrical theory of diffraction*, *Proc. Sympos. Appl. Math.*, 8 (1958), pp. 27–52.
- [17] S. KOGA, *Rotating spiral waves in reaction diffusion systems*, to appear.
- [18] V. I. KRINSKY, *Mathematical models of cardiac arrhythmias*, *Pharmac. Ther. B.*, 3 (1978), pp. 539–555.
- [19] G. H. MARKSTEIN, *Experimental and theoretical studies of flame front stability*, *J. Aero. Sci.*, 18 (1951), pp. 199–209.
- [20] H. MARTINS-FERREIRA, G. DE OLIVEIRO CASTRO, C. J. STRUCHINEA AND P. S. RODRIGUES, *Circling spreading depression in isolated chick retina*, *J. Neurophysics*, 37 (1974), pp. 773–784.
- [21] H. P. MCKEAN, *Nagumo's equation*, *Adv. in Math.*, 4 (1975), pp. 209–223.
- [22] A. S. MIKHAILOV AND V. I. KRINSKY, *Rotating spiral waves in excitable media: the analytical results*, *Physica D*, 9 (1983), pp. 346–371.
- [23] R. MILLER AND J. RINZEL, *The dependence of impulse propagation speed on firing frequency, dispersion for the Hodgkin–Huxley models*, *Biophysics J.*, 34 (1981), pp. 227–259.

- [24] G. R. MINES, *On circulating excitation on heart muscles and their possible relation to tachycardia and fibrillation*, Trans. Roy. Soc. Canada, 4 (1914), pp. 43–53.
- [25] R. M. MIURA, *Nonlinear waves in neuronal cortical structures*, in Nonlinear Phenomena in Physics and Biology, R. H. Enns, B. L. Jones, R. M. Miura and S. S. Rangnekar, eds., Plenum, New York, 1981, pp. 369–400.
- [26] G. K. MOE, W. C. RHEINOLDT AND J. A. ABILDSKOV, *A computer model of atrial fibrillation*, Am. Heart J., 67 (1964), pp. 200–220.
- [27] A. M. PERTSOV, E. A. ERMAKOVA AND A. V. PANFILOV, *Rotating spiral waves in a modified FitzHugh–Nagumo equation model*, Physica 14 D, (1984) pp. 117–124.
- [28] J. RINZEL AND K. MAGINU, *Kinematic analysis of spatio-temporal wave patterns*, Bordeaux, 1984, to appear.
- [29] J. RINZEL AND J. B. KELLER, *Traveling wave solutions of a nerve conduction equation*, Biophysics J., 13 (1973), pp. 1313–1337.
- [30] M. SHIBATA AND J. BURES, *Reverberation of cortical spreading depression along closed loop pathways in rat cerebral cortex*, J. Neurophysics, 35 (1972), pp. 381–388.
- [31] D. TURNBULL, *Phase changes*, in Solid State Physics, 3, F. Seitz and D. Turnbull, eds., Academic Press, New York, 1956.
- [32] J. J. TYSON AND P. C. FIFE, *Target patterns in a realistic model of the Belousov–Zhabotinskii reaction*, J. Chem. Phys., 73 (5) (1980), pp. 2224–2237.
- [33] F. J. L. VAN CAPELLE AND D. DURRER, *Computer simulation of arrhythmias in a network of coupled excitable elements*, Circ. Res., 47 (1980), pp. 454–466.
- [34] G. B. WHITHAM, *Linear and Nonlinear Waves*, Wiley Interscience, New York, 1974.
- [35] N. WEINER AND A. ROSENBLUETH, *The mathematical formulation of the problem of conduction of impulses in a network of connected excitable elements, specifically in cardiac muscle*, Arch. Inst. Cardiol. Mex., 16 (1946), pp. 205–265.
- [36] A. T. WINFREE, *Spiral waves of chemical activity*, Science, 175 (1972), pp. 634–636.
- [37] ———, *The Geometry of Biological Time*, Springer, Berlin, New York, 1980.
- [38] ———, *Rotating solutions to reaction diffusion equations in simply-connected media*, American Mathematical Society–Society for Industrial and Applied Mathematics Proc., 8 (1974), pp. 13–31.
- [39] A. M. ZHABOTINSKY AND A. N. ZHAIKIN, *Autowave processes in a distributed chemical system*, J. Theoret. Biol., 40 (1973), pp. 45–61.
- [40] V. S. ZYKOV AND A. A. PETROV, *Role of the inhomogeneity of an excitable medium in the mechanism of self-sustained activity*, Biophysics, 22 (1977), pp. 307–314.
- [41] V. S. ZYKOV, *Analytical evaluation of the dependence of the speed of excitation wave in a two-dimensional excitable medium on the curvature of its front*, Biophysics, 25 (1980), pp. 906–911.